Prediction of critical current-bending strain relation of Bi2223 composite tape using residual strain of filaments, load-strain curve and geometry of cross-section

AUTHOR(S):

Ochiai, Shojiro; Okuda, H.; Matsubayashi, H.; Mukai, Y.; Shin, J.K.; Iwamoto, S.; Hojo, M.; Sato, M.; Osamura, K.; Mimura, M.

CITATION:

Ochiai, Shojiro ...[et al]. Prediction of critical current-bending strain relation of Bi2223 composite tape using residual strain of filaments, load-strain curve and geometry of cross-section. Physica C: Superconductivity and its Applications 2009, 469(15-20): 1480-1484

ISSUE DATE:

2009-10

URL:

http://hdl.handle.net/2433/85220

Physica C 469(2009)1480-1484 掲載原稿

Prediction of critical current-bending strain relation of Bi2223 composite tape using residual strain of filaments, load-strain curve and geometry of cross-section

S. Ochiai[a,*], H. Okuda[a], H. Matsubayashi[a], Y. Mukai[a], J. K Shin[a], S. Iwamoto[a], M. Hojo[a], M. Sato[b] , K. Osamura[c], M. Mimura[d]

[a] Graduate School of Engineering, Kyoto University, Sakyo-ku, Kyoto 606-8501, Japan.

[b] Japan Synchrotron-radiation Research Institute (JASRI), Kohto, Sayo 679-5198, Japan

[c] Research Institute for Applied Sciences, Sakyo-ku, Kyoto 606-8202, Japan.

[d] Metal Research Center, Furukawa Electric Co. Ltd. Kiyotaki 500, Nikko 321-1493, Japan.

Abstract

A prediction method of the critical current-bending strain relation of the Bi2223 composite tape, which was bent at room temperature and cooled down to 77K for measurement of critical current, was presented. The present method consisted of (a) measurement of residual strain of Bi2223 filaments at room temperature in the sample length direction by the X ray diffraction method, (b) estimation of tensile fracture strain of the filaments from the analysis of the load-strain curve at room temperature, (c) measurement of geometrical factors such as the thickness of the sample and shape of the core by observation of the cross-section with optical microscope, and (d) calculation of the critical current as a function of bending strain by using the measured parameters

mentioned in (a), (b) and (c). The predicted variation of critical current with bending strain by the present approach described well the experimental one.

PACS Classification numbers: 74.25.Ld, 74.72Hs, 74.81Bd

Keywords: Bi2223 composite superconductor, residual strain, fracture strain, critical current, X ray diffraction method

*Corresponding author.

Prof. Shojiro Ochiai

Postal address: Department of Materials Science and Engineering, Graduate School of Engineering, Kyoto University, Yoshida, Sakyo-ku, Kyoto 606-8501, Japan

Phone: +81 75 753 4834

Fax: +81 75 753 4841

E-mail address: shojiro.ochiai@materials.mbox.media.kyoto-u.ac.jp

1. Introduction

It has been known that the critical current of Bi2223/Ag/Ag alloy composite tapes decreases with increasing applied tensile (ε_T) and bending (ε_B) strains beyond the irreversible strain due to the damage evolution of the Bi2223 filaments [1-13]. In the damage evolution process under the applied tensile strain, the residual strain $\varepsilon_{Bi,r}$ of the filaments, which arises during cooling due to the difference in coefficient of thermal expansion among the Bi2223 filaments, Ag and Ag alloy [3,7,9,10,12] and tensile fracture strain $\varepsilon_{Bi,f}$ of the filaments in the sample length direction (current transport direction) play a dominant role in the damage process. Under the applied bending strain, they also play a dominant role since the damage is caused by the tensile strain in the sample length direction [10,13]. However, the damage process under bending strain is different from that under tensile strain, since the exerted tensile strain in the bent sample is dependent on the location and therefore the damage amount is dependent on the shape of the core, as will be shown later in detail. Thus, for description of critical current-bending strain relation, the shape of the core as well as $\varepsilon_{Bi,r}$ and $\varepsilon_{Bi,f}$ values are needed [13].

The aim of the present work is to present a simple approach for prediction of the critical current at 77K of the composite tape bent at room temperature. The present approach consists of (a) measurement of residual strain of Bi2223 filaments at room temperature in the sample length direction by the X ray diffraction method, (b) estimation of tensile fracture strain of the filaments at room temperature from analysis of the load-strain curve measured by the tensile test, in which the residual strain value measured in (a) was taken into consideration, (c) measurement of geometrical factors

such as the thickness of the sample and shape of the core by observation of the cross-section with a conventional optical microscope, and (d) calculation of the critical current as a function of bending strain by using the measured parameters mentioned in (a), (b) and (c). The present approach will be shown to be valid from the comparison of the predicted critical current-bending strain relation with the experimental one.

2. Experimental procedure

2.1 Test sample

The multi-filamentary Bi2223/Ag/Ag alloy composite tape fabricated at Furukawa Electric Co. Ltd, Japan, was used for tests. The thickness and width were 0.27 and 4.2 mm, respectively. The tape was composed of the outer sheath of Ag alloy and the inner core in which the Bi2223 filaments that transport the superconducting current are embedded in Ag, as shown in Fig.1. Fig.1(a) shows the micrograph of the as observed cross-section. When the thickness direction of the micrograph is enlarged by 3 times as in (b), the shape of the core is more clearly found. The boundary of the core is shown with the solid curve, which will be formulated later in 3.3.

2.2 Residual strain measurement

The residual strain of Bi2223 filaments in the composite tape at room temperature was measured by the X ray diffraction method. Details of the procedure have been shown elsewhere [12]. The outline is as follows. As a reference specimen, the strain-free bare Bi2223 filaments, which were extracted from the composite tape by etching away the Ag and Ag alloy with a NH_4OH/H_2O_2 solution, was used. The Bragg peaks of the

strained Bi2223 filaments in the composite and strain-free Bi2223 filaments alone were measured from the former and latter specimens, respectively. The experiment was carried out at the beam line 46XU of a synchrotron-radiation facility, SPring 8, Japan. A strong X-ray from an undulator was monochromatized into a beam of 22keV. The beam size was 0.5x1.0 mm^2. The charge-coupled device (CCD) monitor was used to control the position of the specimen. The peak positions of (200), (220) and (400) planes were used for the present analysis. From the Bragg peak angle of the Bi2223 filaments in the composite tape with residual strain, θ_{comp}, and that of strain free filaments extracted from the composite tape, θ_0, the residual strain of the filaments in the composite was estimated by

$$\varepsilon_{Bi,r} = \frac{1/\sin(\theta_{comp}) - 1/\sin(\theta_0)}{1/\sin(\theta_0)} \qquad (1)$$

2.3 Tensile test

Tensile test was carried out using a universal testing machine (autograph AG-50kNG, Shimadzu, Japan) at a strain rate of $1.6x10^{-4}$/s at room temperature. The strain was measured with a very light couple type extensometer developed by Nyilas [14].

2.4 Critical current measurement of bent samples

The measurement of critical current of bent samples was carried out with the procedure employed in the round robin test of VAMAS (Versailles project on advanced materials and standard)/TWA 16 (Technical working area 16, superconducting

materials) [15]. Bending strain was given at room temperature by pressing the sample with the upper GFRP die to the lower one with the same curvature. The bending strain ε_B (=tensile strain of the outer surface of the composite in the tensile side) was given by $\varepsilon_B = t/(2R)$ where t is the overall thickness of the sample and R is the radius of the die. Six pairs of dies with the radius $R = \infty$ (straight dies), 61.6, 34.0, 22.3, 17.3 and 13.8 mm were used to give bending strain, corresponding to ε_B=0, 0.2, 0.4, 0.6, 0.8 and 1.0% for the present samples. The samples bent at room temperature were cooled down to 77K, at which the critical current I_c was measured with a criterion of 1μV/cm in the self magnetic field. The distance between the voltage taps was 30 mm. After the measurement of the critical current at a given bending strain, the samples were warmed up to room temperature at which the bending strain was raised to the next prescribed one. The samples with increased bending strain were again cooled down to 77K for measurement of critical current. Such a procedure was repeated to obtain the critical current-bending strain relation. In this process, the bending-induced damage took place always at room temperature. The critical current I_c (1μV/cm criterion) - bending strain ε_B was measured for four test specimens. The I_c-value was normalized with respect to the original critical current at ε_B=0, I_{c0}, for each test sample. The normalized critical current, I_c/I_{c0}, of the four test samples at each given bending strain was averaged, and I_c/I_{c0}-ε_B relation was obtained.

3. Results and discussion

3.1 Residual strain of Bi2223 filaments in the composite tape

Figure 2 shows the estimated residual strain ($\varepsilon_{Bi,r}$) values by the X ray diffraction method. The estimated values from the X ray profiles of the (200), (220) and (400) planes were minus, indicating that the Bi2223 filaments had compressive residual strain in the sample length direction. On an average, the $\varepsilon_{Bi,r}$ was estimated to be -0.12%.

3.2. Estimation of residual and yield strains of Ag and Ag alloy and tensile fracture strain of the Bi2223 filaments from the tensile load-strain curve of the composite in combination with the estimated residual strain of the Bi2223 filaments in 3.1.

Figure 3 shows the tensile load (L_T) - strain (ε_T) curve of the composite tape which had been cooled to 77K for pre-check of the critical current and then warmed up to room temperature at Furukawa Electric Co. Ltd. Concerning the deformation and fracture behavior of the samples with such a thermal history, the following stages of deformation and fracture have been found in the load-strain curve in our former work [12]. The present composite tape behaves in a same manner. The overall load-strain curve is shown in Fig.3(a).

Stage I. As the yield strain of Ag is low (0.02% as shown later), Ag in the composite tape, which has been cooled down to 77K and then warmed up to room temperature, is yielded in compression at room temperature [12]. When the composite is pulled in tension, Ag that is yielded in compression deforms elastically with increasing applied strain and then it is yielded in tension. In this stage, Ag, Ag alloy and Bi2223 filaments deform elastically. This stage is in the applied strain range of $0 \leq \varepsilon_T \leq 2\varepsilon_{Ag,y}$ where $\varepsilon_{Ag,y}$ (=0.02%) is the yield strain of Ag.

Stage II. With increasing applied tensile strain beyond stage I, Ag deforms

plastically, while Ag alloy and Bi2223 filaments deform elastically. At the end of this stage, Ag alloy yields at $\varepsilon_T=\varepsilon_{Alloy,y}-\varepsilon_{Alloy,r}$ where $\varepsilon_{Alloy,y}$ and $\varepsilon_{Alloy,r}$ are the yield- and residual strains of Ag alloy, respectively. Thus, this stage is in the applied strain range of $2\varepsilon_{Ag,y}\leq\varepsilon_T\leq \varepsilon_{Alloy,y}-\varepsilon_{Alloy,r}$.

Stage III. With further increasing applied strain beyond stage II, Ag and Ag alloy deform plastically and only Bi2223 filaments deform elastically. In this stage, the Bi2223 filaments are fractured at $\varepsilon_T=\varepsilon_{Bi,f}-\varepsilon_{Bi,r}$. In the fracture evolution process, the filaments are fractured more with increasing ε_T, resulting in multiple fracture state since the stress is transferred even to the once fractured filaments [16,17]. Due to such continual fractures of the filaments, the load bearing capacity of the Bi2223/Ag/Ag alloy composite tape is reduced in comparison with that without fracture of filaments. Accordingly the slope of the load-strain curve is reduced [5, 13]. The portion of load-strain curve in stage III, surrounded by the rectangle in Fig.3(a), is presented in Fig.3(b) at high magnification. The slope reduction at the end of this stage is clearly found in Fig.3(b).

From the analysis of stages I and II in the load-strain curve (Fig.3(a)), the residual($\varepsilon_{Ag,r}$)- and yield($\varepsilon_{Ag,y}$)-strains of Ag and the residual($\varepsilon_{Alloy,r}$)- and yield($\varepsilon_{Alloy,y}$)-strains of Ag alloy can be estimated, respectively, and also from the analysis of stage III, the fracture strain $\varepsilon_{Bi,f}$ of Bi2223 filaments can be estimated in a following manner.

(A) Residual ($\varepsilon_{Ag,r}$)- and yield($\varepsilon_{Ag,y}$) - strains of Ag

The applied tensile at the deviation from stage I to II, corresponding to $2\varepsilon_{Ag,y}$, is read to be 0.04%. Accordingly, the yield strain $\varepsilon_{Ag,y}$ of the present sample is 0.02%. As

Ag is soft, it is approximated to be an elastic-perfect plastic body. Under such an approximation, the elastic component of the residual strain of Ag, $\varepsilon_{Ag,r}$ (= $-\varepsilon_{Ag,y}$), is estimated to be -0.02%.

(B) Residual ($\varepsilon_{Alloy,r}$)- and yield ($\varepsilon_{Alloy,y}$)- strains of Ag alloy

The slope of the stress-strain curve in the plastic deformation region of metals is far lower than the Young's modulus. Approximating the Ag alloy (as well as Ag) as the elastic-perfect plastic body and noting the cross-sectional area as A and the Young's modulus E, the slopes $E_{c,I}A_c$, $E_{c,II}A_c$, $E_{c,III}A_c$ of the load-strain curve in stages I, II and III (Fig.3) are approximately given by [12]

$$E_{c,I}A_c = E_{Bi}A_{Bi} + E_{Ag}A_{Ag} + E_{Alloy}A_{Alloy} \quad \text{(Stage I)} \quad (2)$$

$$E_{c,II}A_c = E_{Bi}A_{Bi} + E_{Alloy}A_{Alloy} \quad \text{(Stage II)} \quad (3)$$

$$E_{c,III}A_c = E_{Bi}A_{Bi} \quad \text{(Stage III)} \quad (4)$$

where the subscripts c, Bi, Ag and Alloy refer to composite tape, Bi2223 filaments, Ag and Ag alloy, respectively, and the subscripts I, II and III refer to stages I, II and III, respectively. From the slope in each stage in Fig.3, the $E_{c,I}A_c$, $E_{c,II}A_c$ and $E_{c,III}A_c$ were read to be 78.5, 59.2 and 38.5 kN, respectively. Substituting these measured values into Eqs.(2) to (4), the $E_{Bi}A_{Bi}$, $E_{Ag}A_{Ag}$ and $E_{Alloy}A_{Alloy}$ were estimated to be 19.6, 20.7 and 38.5 kN, respectively. As the residual stresses are balanced, the sum of the residual stresses of the constituents is zero, which is expressed by,

$$\varepsilon_{Ag,r}E_{Ag}A_{Ag} + \varepsilon_{Alloy,r}E_{Alloy}A_{Alloy} + \varepsilon_{Bi,r}E_{Bi}A_{Bi} = 0 \quad (5)$$

Substituting the values mentioned above ($\varepsilon_{Ag,r}$=-0.02%, $\varepsilon_{Bi,r}$=-0.12%, $E_{Ag}A_{Ag}$□=19.6 kN, □$E_{Alloy}A_{Alloy}$=20.7 kN and $E_{Bi}A_{Bi}$=38.5 kN) into Eq.(5), we had the residual strain of Ag alloy, $\varepsilon_{Alloy,r}$=0.24%. As shown in Fig.3(a), Ag alloy in the composite showed yielding at ε_T=0.10%. The yield strain of Ag alloy, $\varepsilon_{Alloy,y}$, is given by ε_T(0.10%)+$\varepsilon_{Alloy,r}$(0.24%) =0.34%. The yield stress is calculated to be 310 MPa for the reported Young's modulus value 88 GPa [18], which is similar to the reported value of 330 MPa estimated from the stress-strain curve of the Ag alloy itself [18].

(C) Fracture strain of the Bi2223 filaments

When the Bi2223 filaments are fractured at the end of stage III, the load bearing capacity of the composite tape is reduced in comparison with that of the composite without fracture of the filaments. Accordingly, the load carrying capacity deviates from the extrapolation of the load-strain relation of the undamaged region (broken line), as has been shown in Fig.3(b). It is judged that the Bi2223 filaments are fractured at the applied tensile strain ($\varepsilon_{T,f}$) around 0.20%. As the $\varepsilon_{T,f}$ corresponds to $\varepsilon_{Bi,f}$ - $\varepsilon_{Bi,r}$, the $\varepsilon_{Bi,T}$ value is estimated to be 0.08% for $\varepsilon_{Bi,r}$=-0.12% obtained in 3.1. The estimated value is similar to the reported value of around 0.1% for Bi2223 filaments [5, 10, 12].

3.3 Prediction of critical current (I_c/I_{c0}) - bending strain (ε_B) relation and comparison of the predicted relation with the experimental one

For prediction of the I_c/I_{c0}-ε_B relation, the model proposed in our former work [13] was employed, in which the I_c/I_{c0} has been formulated as a function of ε_B, $\varepsilon_{Bi,r}$, $\varepsilon_{Bi,f}$ and

the structural parameters (overall thickness of the sample, shape and size of the core in which the Bi2223 filaments that transport the superconducting current). The outlines of the procedure for analysis and the employed formulations are presented below. Details of the derivation of formulations and the approximations used in the modeling have been shown elsewhere [13].

The cross-section taken from Fig.1 and the relation of bending strain to damage front are schematically presented in Fig.4. Under the applied bending strain, the tensile strain exerted on the filaments in the sample length direction is dependent on the location; the exerted tensile strain increases with the distance from the neutral axis [13]. Thus the filaments most apart from the neutral axis tends to be fractured first. Then, at increased bending strain, the filaments beneath the most apart one are fractured. As the damage of the Bi2223 filaments existing in the core causes the reduction in critical current, it is needed to formulate the shape. Taking the width- and thickness- directions of the composite tape as x and y, respectively, and the center of the composite tape as x=y=0 (Fig.4), and noting the y coordinate of the boundary abcd of the core as y_{core}, we formulated y_{core} as a function of x by a 9th order polynomial for the present sample. The length unit is mm.

$$\left.\begin{aligned} \text{ab:} y_{core} &= 0.0856769 + 0.0248085x + 0.602842x^2 + 2.46881x^3 \\ &\quad + 5.41614x^4 + 7.47217x^5 + 6.52648x^6 + 3.47349x^7 \\ &\quad + 1.02285x^8 + 0.127373x^9 \qquad \text{for } -1.95 \le x \le 0 \\ \text{bc: symmetry with ab with respct to } y \text{ axis} & \\ \text{adc: symmetry with abc with respect to } x \text{ axis} & \end{aligned}\right\} \quad (6)$$

When the bending strain ε_B reaches the irreversible strain $\varepsilon_{B,irr}$, the damage to

reduce the critical current takes place first at the outermost filaments at the maximum value of y_{core}, $y_{core,max}$(Fig.4). The $y_{core,max}$ value was 0.099 mm. When the bending strain ($\varepsilon_B \geq \varepsilon_{B,irr}$) is raised from $\varepsilon_{B,i}$ to $\varepsilon_{B,i+1}$, the damage front y_f moves from $y_{f,i}$ to $y_{f,i+1}$, resulting in reduction of the cross-sectional area of the current transporting Bi2223 filaments and therefore resulting in reduction of critical current. According to the preceding modeling work [13], the irreversible strain $\varepsilon_{B,irr}$ and the normalized critical current I_c/I_{c0} as a function of bending strain ε_B are given by

$$\varepsilon_{B,irr} = \left(\frac{t/2}{y_{core,max}} \right) (\varepsilon_{Bi,f} - \varepsilon_{Bi,r}) \qquad (7)$$

$$\frac{I_c}{I_{c0}} = 1 \qquad \text{for } \varepsilon_B \leq \varepsilon_{B,irr} \qquad (8)$$

$$\frac{I_c}{I_{c0}} = 1 - \int_{-W_{core}/2}^{W_{core}/2} \left[y_{core} - \left\{ \frac{(t/2)(\varepsilon_{Bi,f} - \varepsilon_{Bi,r})}{\varepsilon_B} \right\} \right] dx / S_{core} \qquad \text{for } \varepsilon_{B,irr} \leq \varepsilon_B \square \qquad (9)$$

where W_{core} and S_{core} are the width and cross-sectional area of the core, respectively. Substituting y_{core} expressed by Eq.(6), the measured values of the geometrical parameters ($y_{core,max}$=0.099 mm, W_{core}=3.91 mm, t=0.270 mm and S_{core} =0.602 mm^2) and the residual- ($\varepsilon_{Bi,r}$ = -0.12 %) and fracture ($\varepsilon_{Bi,f}$=0.08%) strains of the filaments estimated in 3.1 and 3.2, respectively, into Eqs.(7), (8) and (9), we calculated the variation of I_c/I_{c0} as a function of ε_B.

Figure 5 shows the calculated and measured change of the normalized critical current I_c/I_{c0} with increasing bending strain ε_B. The open circles show the average and the error bars show the minimum and maximum of the measured I_c/I_{c0} values of four

samples. The experimentally measured I_c/I_{c0}-ε_B relation was described well.

The agreement of the predicted relation with the experimental one suggests that the present approach is a useful tool for prediction of I_c/I_{c0}-ε_B.

4. Conclusions

(1) The residual strain of the Bi2223 filaments at room temperature in the sample length direction of the Bi2223/Ag/Ag alloy composite tape was estimated to be -0.12% by the X ray diffraction method in which the filaments extracted from the composite were used as the stress free-reference sample.

(2) From the analysis of the tensile load - strain curve in combination with the residual strain value of the Bi2223 filaments, the residual elastic strains of Ag and Ag alloys in the composite tape were estimated to be -0.02 and 0.24%, and the intrinsic yield strains to be 0.02 and 0.34%, respectively. Also the tensile fracture strain of the Bi2223 filaments was estimated to be 0.08%.

(3) The change of critical current at 77K with bending strain given at room temperature was predicted by using the measured residual strain of Bi2223, tensile fracture strain of Bi2223 and the structural factors of the composite tape such as the overall thickness, outermost position of the core at which the fracture of the filaments takes place first and shape of the core. The predicted variation of the critical current with bending strain described well the experimental result.

Acknowledgement

This research was supported by the grant-in-aid of The Ministry of Education, Culture, Sports, Science and Technology, Japan (no. 18106011).

References

[1] H. Kitaguchi, K. Itoh, H. Kumakura, T. Takeuchi, K. Togano, H. Wada, IEEE Trans. Appl. Supercond.11 (2001) 3058.

[2] H. J. N. van Eck, K. Vargast, B. ten Haken, H. H. J. ten Kate, Supercond. Sci. Technol. 15 (2002) 1213.

[3] R. Passerini, M. Dhalle, B. Seeber, R. Flükiger, Supercond. Sci. Technol. 15 (2002) 1507.

[4] S. J. Sun, W. Liu, X. P. Chen, M. Y. Li, Z. Han, Supercond. Sci. Technol. 16 (2003) 984.

[5] S. Ochiai, T. Nagai, H. Okuda, S. S. Oh, M. Hojo, M. Tanaka, M. Sugano, K. Osamura, Supercond. Sci. Technol. 16 (2003) 988.

[6] K. Katagiri, H. S. Shin, K. Kasaba, T. Tsukinokizawa, K. Hiroi, T. Kuroda, K. Itoh, H. Wada, Supercond. Sci. Technol. 16 (2003) 995.

[7] H. S. Shin, K. Katagiri, Supercond. Sci. Technol. 16 (2003) 1012.

[8] H. J. N. van Eck, D. C. van der Laan, M. Dhallé, B. ten Haken, H. H. J. ten Kate, Supercond. Sci. Technol. 16 (2003) 1026.

[9] M. Hojo, M. Nakamura, T. Matsuoka, M. Tanaka, S. Ochiai, M. Sugano, K. Osamura, Supercond. Sci. Technol. 16 (2003) 1043.

[10] S. Ochiai, N. Miyazaki, D. Doko, T. Nagai, M. Nakamura, H. Okuda, S. S. Oh, M. Hojo, M. Tanaka, K. Osamura, J. Nuclear Mater. 329-333 (2004) 1585.

[11] K. Katagiri, T. Kuroda, H. S. Shin, K. Hiroi, K. Itoh, H. Wada, Physica C 426-431 (2005) 1200.

[12] S. Ochiai, H. Rokkaku, K. Morishita, J. K. Shin, S. Iwamoto,H. Okuda, M. Hojo, K. Osamura, M. Sato, A. Otto, E. J. Harley, A. Malozemoff, Supercond. Sci. Technol. 20 (2007) 202.

[13] S. Ochiai, T. Matsuoka, J. K. Shin, H. Okuda, M. Sugano, M Hojo, K. Osamura, Supercond. Sci. Tecnol. 20 (2007) 1076.

[14] A. Nyilas, Supercond. Sci. Technol. 18 (2005) S409.

[15] T. Kuroda, K. Itoh, K. Katagiri, W. Goldacker, W. Haessler, B. ten Haken, M. Kiuchi, N. Noto, S. Ochiai, S. Otabe, H. S. Shin, J. Sosnowski, H. Weijers, H. Wada, K. Kumakura, Physica C 425 (2005) 111.

[16] S. Ochiai, M. Hojo, J. Mater. Sci. 31 (1996) 3861.

[17] S. Ochiai, T. Sawada, M. Hojo, J. Sci. Eng. Comp. 6 (1997) 63.

[18] M. Sugano, K. Osamura, A. Nyilas, Physica C 412-414 (2004) 1114.

Figure captions

Fig.1 Transverse cross-section of the composite tape. (a) Optical micrograph in as observed state and the shape of the core. (b) Deformed optical micrograph, where the thickness direction is 3 times enlarged from the as-observed one in (a). The solid curve in (b) shows the shape of the core, which will be formulated later in 3.3.

Fig.2 The measured values of the residual strain $\varepsilon_{\mathrm{Bi,r}}$ of the Bi2223 filaments in the composite tape from the (200), (220) and (400) planes.

Fig.3 Measured tensile load (L_{T}) -strain (ε_{T}) curve at room temperature. The part surrounded by the rectangle in (a) is presented in (b) at high magnification.Fig.4 Schematic representation of the geometry of the cross-section of the composite tape in relation to the damage extension. Damage occurs first at the outermost filaments at the maximum value of y_{core}, $y_{\mathrm{core,max}}$ when the bending strain ε_{B} reaches $\varepsilon_{\mathrm{B,irr}}$. When the bending strain ε_{B} is raised from $\varepsilon_{\mathrm{B,irr}}$ to $\varepsilon_{\mathrm{B},i}$ and then to $\varepsilon_{\mathrm{B},i+1}$, the damage front y_{f} moves from $y_{\mathrm{core,max}}$ to $y_{\mathrm{f},i}$ and then to $y_{\mathrm{f},i+1}$

Fig.5 Comparison of the predicted relation of the normalized critical current $I_{\mathrm{c}}/I_{\mathrm{c0}}$ to the bending stain ε_{B} with the measured one. The solid curve shows the predicted relation. The open circle, upper bar and lower bar at each applied bending strain show the average, the highest and lowest values of 4 tested samples, respectively.

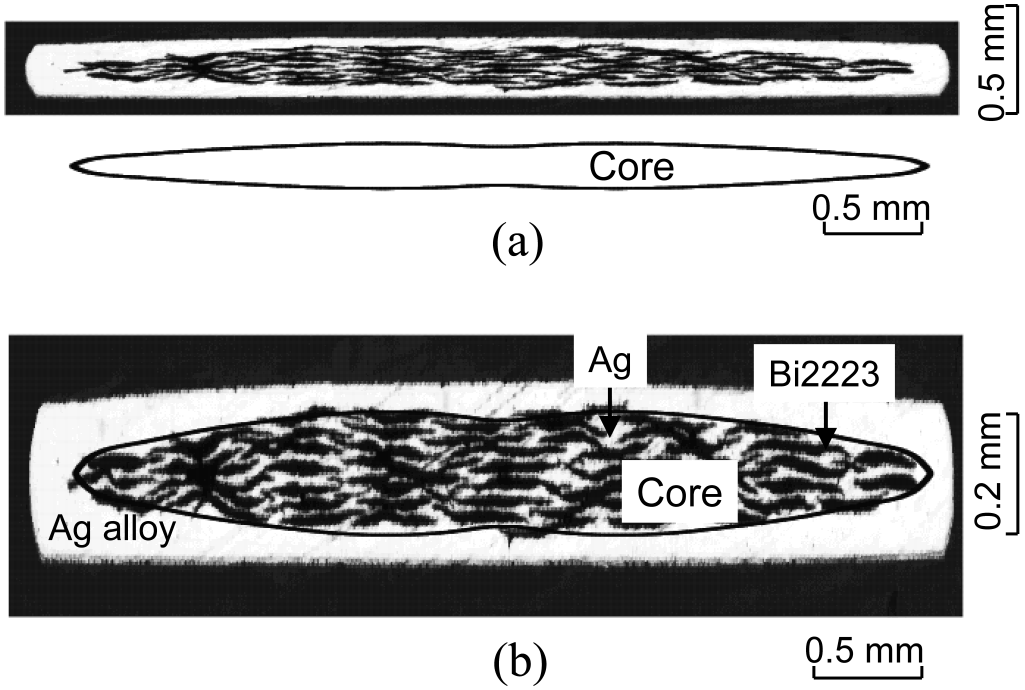

Fig.1

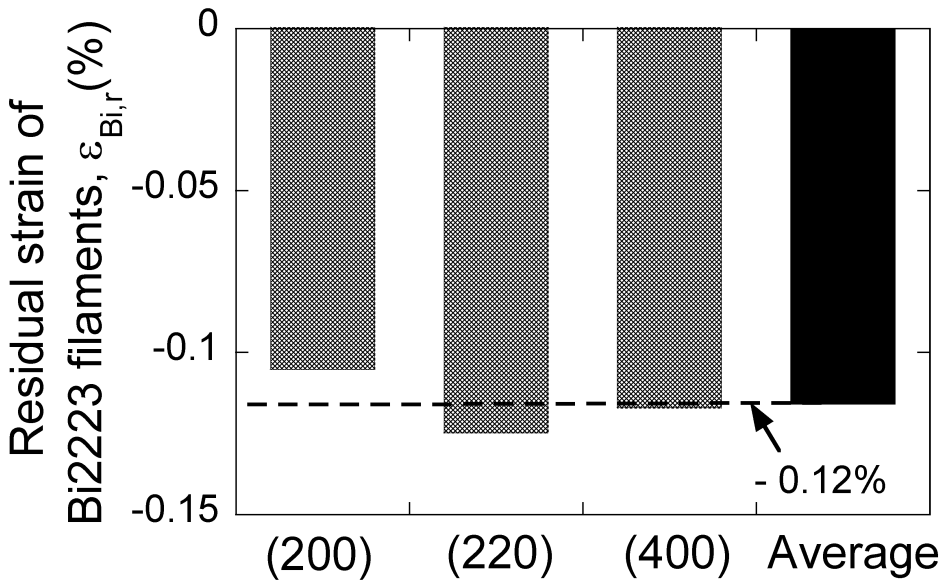

Fig.2

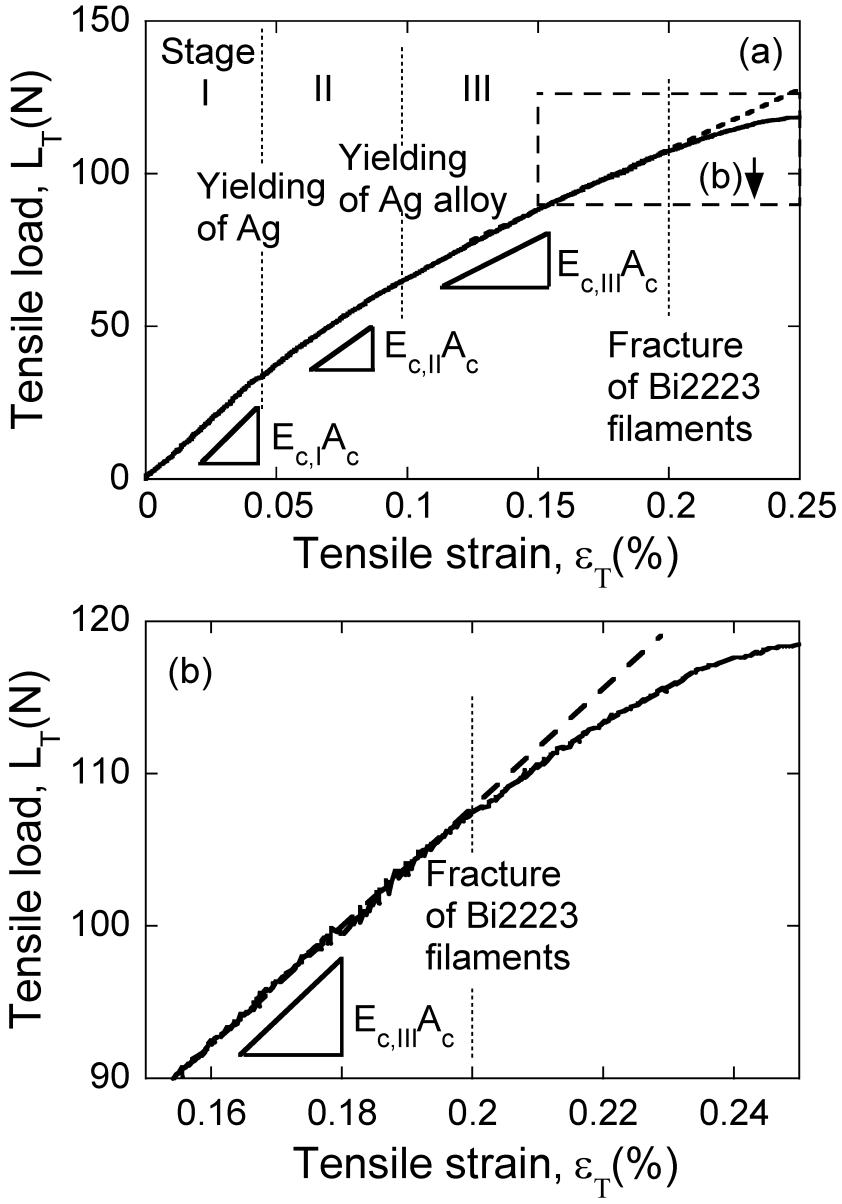

Fig.3

Fig.4

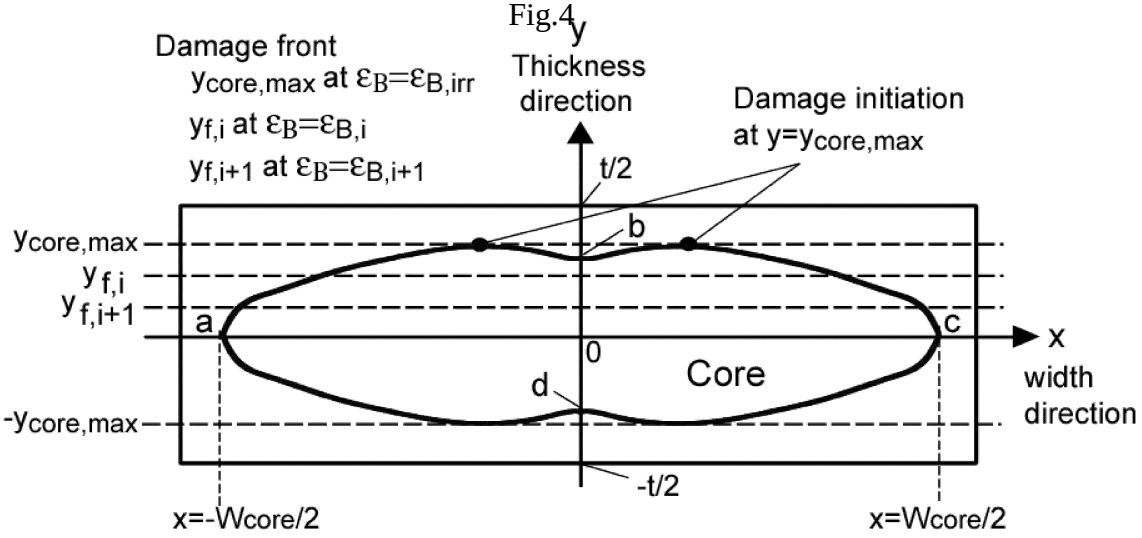

Fig.5